Influences of Mach Number and Flow Incidence on Aerodynamic Losses of Steam Turbine Blade

Seok-Jae, Yoo*
Yong-in Song-Dam College
Wing Fai Ng
Mechanical Engineering Department, Virginia Polytechnic & State University

An experiment was conducted to investigate the aerodynamic losses of high pressure steam turbine nozzle (526A) subjected to a large range of incident angles (−34° to 26°) and exit Mach numbers (0.6 and 1.15). Measurements included downstream Pitot probe traverses, upstream total pressure, and endwall static pressures. Flow visualization techniques such as shadowgraph and color oil flow visualization were performed to complement the measured data. When the exit Mach number for nozzles increased from 0.9 to 1.1 the total pressure loss coefficient increased by a factor of 7 as compared to the total pressure losses measured at subsonic conditions ($M_2<0.9$). For the range of incidence tested, the effect of flow incidence on the total pressure losses is less pronounced. Based on the shadowgraphs taken during the experiment, it' s believed that the large increase in losses at transonic conditions is due to strong shock/ boundary layer interaction that may lead to flow separation on the blade suction surface.

Key Words : Incidence, Mach Number, Total Pressure Loss, Flow Visualization

Nomenclature

C : Chord
O : Throat
S : Pitch
C/S : Solidity
O/S : Gauging
α : Flow angle
β : Metal angle
i : Incidence ($\beta_1-\alpha_1$)
PS : Pressure side
SS : Suction side
tmax : Maximum blade thickness
P_o : Stagnation pressure
P_s : Static pressure
T_o : Stagnation temperature
T_s : Static temperature
P_d : Differential total pressure, $P_{o1}-P_{o2}$
M : Mach number
ρ : Density
V : Velocity
ω : Mass averaged total pressure loss coefficient
τ : Mass averaged kinetic energy loss coefficient

Subscripts

1 : Inlet
2 : Exit
i : Isentropic

* Corresponding Author,
TEL : +82-335-330-9211
Yong-in Song-Dam College, 571-1, Mapyung-dong Yongin-si, Kyunggi-do 449-040, Korea. (Manuscript Received August 4, 1999; Revised January 24, 2000)

1. Introduction

In the power generation industry gas turbines and steam turbines are widely used for generating power. These industrial machines are capable of producing power in hundreds of megawatts. The efficiency of a turbine is largely dependent on its aerodynamic performance.

Nozzles and rotors are designed to operate at a certain condition. However, in actual applications, they are operated at off-design conditions

quite frequently. This change results in the inlet flow entering the various stages in the turbine to be off incidence.

Profile losses generally increase, which leads to the decline in the overall efficiency of the turbine.

Cascade tests have been carried out over the years to determine aerodynamic losses in turbomachines. Although the results from such tests are not as accurate as the data obtained from the tests conducted on the operating turbomachine, cascades provide a blade designer with an economical alternative to determine the aerodynamic efficiency of the blades under various operating conditions. In the late eighties, Hodson and Dominy(1987), Goobie et al. (1989), and Venkatrayulu et al. (1989) published articles demonstrating the effect of incidence on the performance of the turbine rotor blades.

Experiments were carried out in a transonic test -section to investigate the aerodynamic losses of the sets of steam turbine nozzles operating at design and off-design incidence in transonic flow. Incidence angles are varied from -34 ° to 26 ° for the cascade tests. The test at such large range of incident angles is uncommon in linear cascade tests performed by most researchers. Pressure measurements such as total pressure and wall static pressure are used to compute the loss coefficient. The loss coefficient is then compared at various incidences at a specific exit Mach number.

2. Background

2.1 Shock structure and loss mechanisms

Shock is the form of physical discontinuity and has the appearance of thin viscous layers. It is formed at the trailing edges when the throat opening is choked. Stagnation enthalpy is unchanged across this discontinuity. Usually a fish-tail shock will be evident near the trailing edge when the exit flow's Mach number exceeds unity. This shock will progress from a weak shock such as a Mach wave to stronger normal shock. Subsequently the normal shock transforms into an oblique shock when the Mach number is further increased. The shock formed on the pressure surface will impinge onto the suction surface of the blade below and is reflected back as a shock. The incident shock on the surface of the blade below and is reflected back as a shock. The incident shock on the suction side boundary layer will produce a pressure rise, causing boundary layer growth. The viscous layer near the shock impingement location has to gain momentum to overcome the pressure rise in that region. Interacting with free stream, the viscous layer increases its momentum and thickness.

At subsonic exit flows, the profile loss coupled with mixing loss are the main components accounting for the total loss. Friction raises the entropy and internal energy of the boundary layer while lowering its stagnation pressure. As the flow exits the trailing edge of blades, the wake interacts rapidly with the free stream. Transonic exit flows are associated with higher overall losses as shock waves start to form at the trailing edges.

This form of loss is attributed to Mach number effects. The initial formation of week normal shocks has negligible effect on the shock loss and the exit flow has a sub-unity Mach number. Significant shock losses are recorded when the exit flow Mach number exceeds unity (Lakshminarayana, 1996).

2.2 Effects of incidence

The primary focus of this investigation is the effect of incidence on the total loss. Turbine blades are usually designed to perform at the optimum level when the approaching flow is at the design condition (ie, zero incidence at the leading edge). Some blades in industry are designed to perform at off-incidence, which means the design incidence has a value other than zero.

Incidence arises when the turbine is required to operate at off-design conditions such as idling, variable speed and varying loading. In steam turbine terminology, incidence is defined as the difference between the inlet blade angle and the inlet flow angle. All angles are measured with respect to the tangential plane at the leading edge. For gas turbines, the angles are measured from the axial plane.

The effects of incidence on the total loss vary

with different blade profile and geometry. Incidence loss is strongly affected by the leading edge geometry, the nose shape will determine the possibility and extent of flow separation (Chen, 1987). The trend of profile loss coefficient against the variation if incidence for impulse and reaction turbine blades were investigated in the 1950's (Ainley, 1948) The exit flow angle is however unaffected by incidence and the turning angle remains constant. Total loss will hence increase as incidence increased or decreased.

3. Experimental Methods

3.2 Wind tunnel facility

The wind tunnel is a blow-down type facility. A four-stage reciprocating compressor is used to pressurize air in storage tanks. A power control panel located in the laboratory is used to control the storage tank pressure and to activate the blow-down sequence. Upon discharge from the storage tanks, the cool air passes through an activated-aluminum dryer to de-humidify the air. Safety valve and control valve is used to maintain constant total pressure upstream of the test-section. Flow in the duct on entering the test-section is straightened via flow straighteners and a mesh-wired frame is installed to provide uniform flow. When the tunnel is started this butterfly valve will automatically adjusted itself to maintain constant mass flow and total pressure as specified by tunnel control computer. Typically the valve takes 5 seconds to achieve constant upstream pressure and is able to maintain constant mass flow rate for 15 seconds. Fig. 1 shows the structure of blow-down wind tunnel facility.

3.2 Test section

A picture of the test-section used in the experiments is shown in Fig. 2. Aluminum blocks located around the cascade guide the flow at the inlet and exit of the test section. The inlet blocks ensure that flow is parallel at the inlet of the cascade. The cascaded blades are mounted on circular plexiglass (one inch thick) with a dowel pin and a hex screw. This fixture is then mounted onto the test-section with external aluminum plates and clamps for sturdiness. Using an alignment pin fixed onto the test-section, the cascade can be rotated to achieve various inlet flow incidences. A probe traverse driven by a 10-watt stepper motor is utilized to make pressure measurements at various exit planes of the cascade.

Table 1 Blade specification

Type	526A
Chord (in)	2.01
Pitch (in)	1.5
Inlet Blade Angle, β_1	76.4°
Exit Flow Angle, α_2	11.54°
Solidity (c/s)	1.34
Gauging (o/s)	0.2

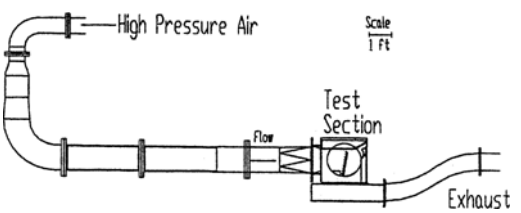

Fig. 1 Blow-down wind tunnel

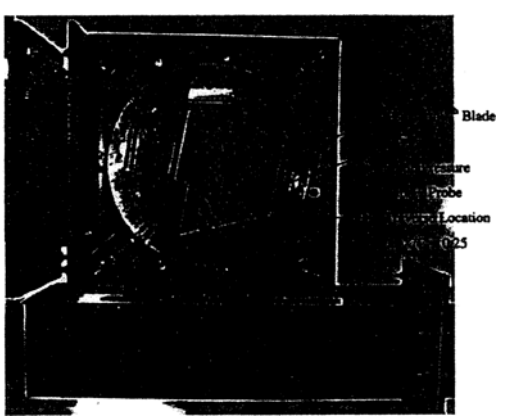

Fig. 2 Instrumented test section

3.3 The nozzle studied

The nozzle used in the high-pressure stage of steam turbines was tested using the current transonic test-section. The inlet blade angle for the nozzle is 75°, and the exit angle is 12°. The nozzle is designed to operate at Mach 0.5. The nozzles used for the cascade test are all six inches in span.

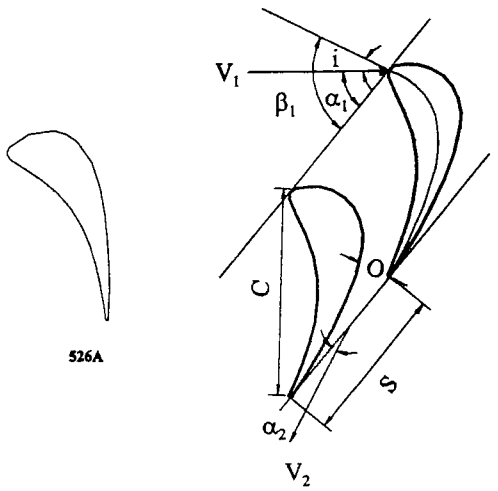

Fig. 3 Blade profiles of tested nozzle

Nozzles are replicated at the high pressure stage without change in their basic profile. Figure 3 displays the dimensions of the nozzle and its respective profiles and illustrates the essential parameters used in defining blade geometry.

4. Data Acquisition and Data Reduction

Aerodynamic measurements are made to obtain data to investigate the variation of losses with different incidence. Upstream total pressure measurement is conducted using a stationary Pitot probe positioned at approximately one foot ahead of the test-section. A probe is mounted at 0.5 inch from the exit plane of the cascade to obtain downstream pressure data. Static measurements were made by mounting taps on the walls of the test-section. The size of the static holes is 1/16 inches in diameter and they are spaced at 0.2-0.3 inches intervals. Each blade passage contains 6-7 pressure taps.

Data acquisition for each tunnel run is performed a high speed data acquisition system (Lecroy) and an independent pressure measurement system. The data obtained by the Lecroy are the upstream total pressure and total temperature, the differential pressure between upstream and the probe and the displacement of the traverse. Each tunnel run has a standard time of approximately 25 seconds. Data are acquired after 5 seconds to let the upstream pressure stabilize. The data acquisition system is set for collecting data with 20-second period and 1000 points of data are collected in each tunnel run. A schematic diagram of the data acquisition procedure is displayed in Fig. 4. Two forms of loss coefficients are determined using the data obtained though the aerodynamic measurements made in the blade passage between the 6th and 8th blades in the cascade. These loss coefficients are pressure loss coefficient and kinetic loss coefficient. The mass averaged form of the pressure loss coefficient and the kinetic loss coefficient over the two blade pitches are given in Eqs. (1) and (2), respectively.

$$\omega=\left[\frac{\int((P_{01}-P_{02})/P_{01})\,\rho_2 V_2 dy}{\int \rho_2 V_2 dy}\right] \tag{1}$$

$$\tau=\left[\frac{\int(1-(V_2-V_{2i})^2)\,\rho_2 V_2 dy}{\int \rho_2 V_2 dy}\right] \tag{2}$$

Static pressure readings at each location P_{2j} taken during the 12-seconds data acquisition time is averaged to obtain a time dverage static pressure reading P_{2js}. The subscript represents the location of the static taps and the probe traverse along the exit tangential plane. This form of average is acceptable, as the variation in static pressure reading over time isn't significant. Upon matching the averaged the static pressure at each wall tap with the downstream probe traverse pressure, the exit Mach number at the location is calculated using the following equation

$$P_{o2j}/P_{2j}=\left[1+\frac{\gamma-1}{2}M_{2j}^2\right]^{\frac{\gamma}{\gamma-1}} \tag{3}$$

When evaluating the isentropic Mach number an equation similar to (3) is used except that the term P_{o2j} is replaced by P_{o1}

From the measured upstream total temperature, the downstream static pressure is evaluated using Eq. (4) assuming that the stagnation temperature $T_{o2}=T_{o1}$.

$$T_{o2}/T_{2j}=1+\frac{\gamma-1}{2}M_{2j}^2 \tag{4}$$

The local density at the wall pressure taps is

determined by the ideal gas law that states

$$\rho_j = \frac{P_{2j}}{RT_{2j}} \tag{5}$$

And the local exit velocity is determined by the speed of sound relation in equation (6)

$$V_{2j} = \frac{M_{2j}}{\sqrt{\gamma RT_{2j}}} \tag{6}$$

A correction formula is necessary to correct the data obtained when the probe traverse experiences supersonic flows or when the following condition is met.

$$P_{2j}/P_{o1} < 0.528 \tag{7}$$

With conditions mentioned above a bow shock is formed at the nose of the probe. The pressure measured by the probe is not representative of flow behavior at that point due to the pressure of the bow shock. Rayleigh supersonic Pitot tube formula is used to correct the calculated exit Mach number and the measured pressure.

$$P_{o2j}/P_{2j} = \left[\frac{\gamma+1}{2} M_{2j}^2\right]^{\frac{\gamma}{\gamma-1}} / \left[\frac{2\gamma}{\gamma+1} M_{2j}^2 - \frac{\gamma-1}{\gamma+1}\right]^{\frac{1}{\gamma-1}} \tag{8}$$

This formula is valid under the assumption that the wall static taps measured the static pressure upstream of the bow shock. M_{2j} is the corrected Mach number using the formula above. The corrected downstream total pressure is evaluated using Eq. (1) with the corrected Mach number. The exit density and velocity have to be determined too.

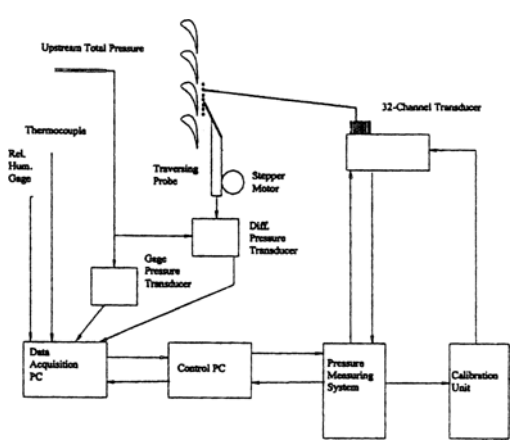

Fig. 4 Schematic diagram for data acquisition

5. Uncertainty Analysis

The experimental uncertainties for the cascade test consist of two types. The first being the uncertainty arising from the accuracy of data acquisition equipment such as pressure transducers and thermocouples. Secondly, due to aperiodicity of the exit flow, the averaged loss coefficient of two blade passage has uncertainty too.

The first source of error from the uncertainty of instruments is reflected on the measured and calculated parameters such as total pressure, differential pressure, static pressure Mach numbers, and loss coefficient. The uncertainty due to the instrument error are:

$$\begin{aligned} \delta P_{o1} &= \pm 0.036 \text{ psi} \\ \delta P_s &= \pm 0.03 \text{ psi} \\ \delta P_d &= \pm 0.01 \text{ psi} \\ \delta T_{o1} &= \pm 1 \text{ K} \end{aligned} \tag{9}$$

Uncertainty for the calculated loss coefficient is a function of the following parameter,

$$\delta\omega = F(\delta P_{o1}, \delta P_d, \delta P_s, \delta T_{o1}) \tag{10}$$

Uncertainty for the exit Mach number is a function of,

$$\delta M_2 = F(\delta P_{o1}, \delta P_d, \delta P_s) \tag{11}$$

The uncertainties for the loss coefficient and Mach numbers are

$$\begin{aligned} \delta\omega &= \pm 0.036\% \\ \delta M_2 &= \pm 0.83\% \end{aligned} \tag{12}$$

Aperiodicity in the exit flow behind the blade passages contributes to the uncertainty in the averaged loss coefficient and averaged exit Mach numbers of the two blade passage measured. These uncertainties are derived from the absolute difference between the measured quantities from the two blade passages and the averaged value from the two blade passages The range of uncertainties due to apeoriodicity at all exit Mach numbers and incident angles are,

$$\begin{aligned} \delta\omega &= \pm 2.93\% \\ \delta M_2 &= \pm 0.66\% \end{aligned} \tag{13}$$

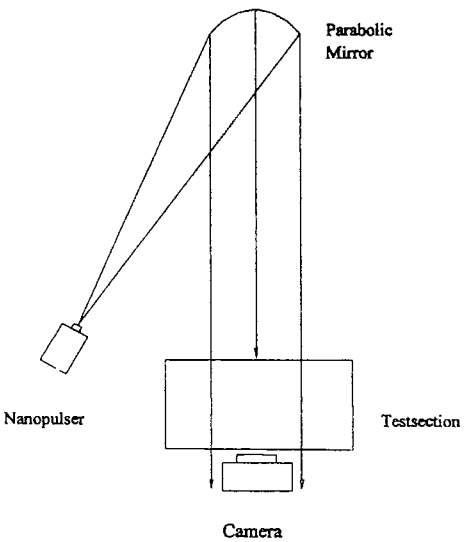

Fig. 5 Setup for shadow photography

6. Shadowgraph and Color Oil Flow Visualization

Shadowgraph photography is an essential flow visualization technique for investigating flows in cascades. The main characteristic of this method

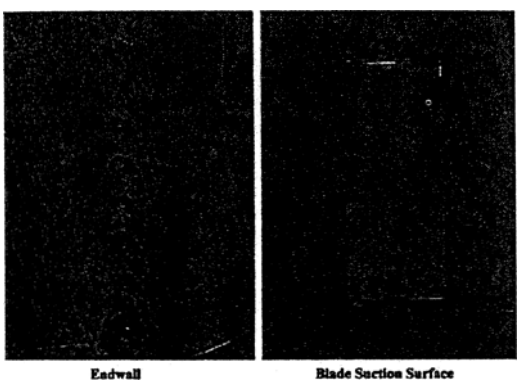

Fig. 6 Color oil flow visualization, I=−4°, Mach=0.6

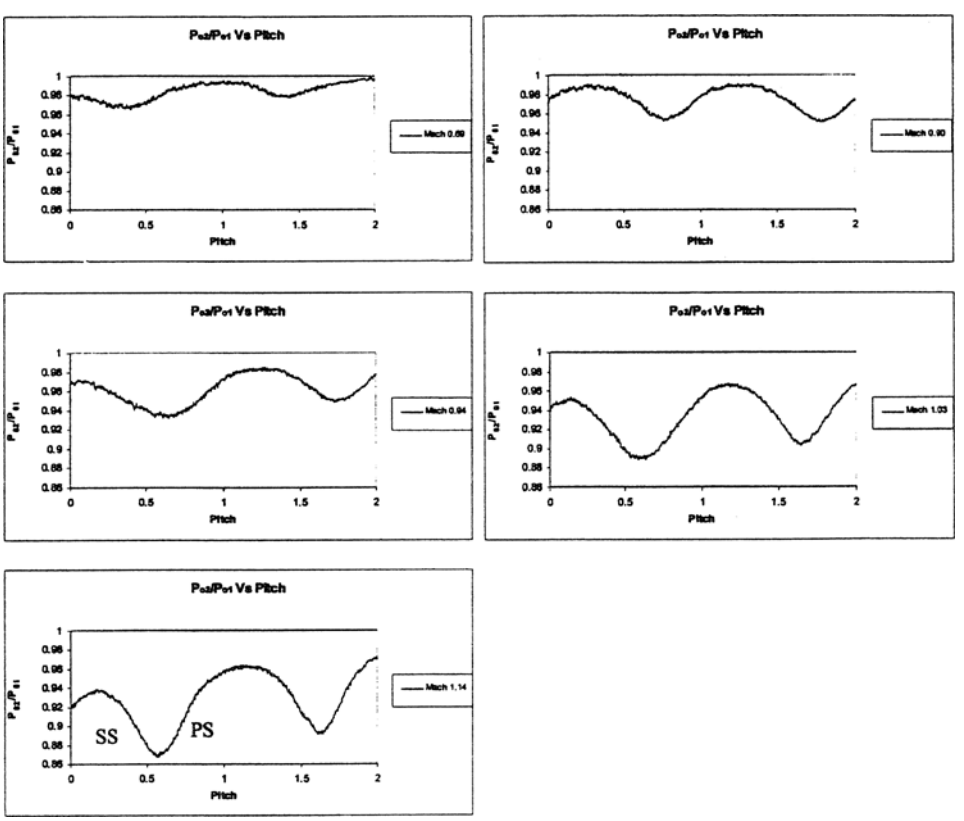

Fig. 7 Pressure ratio at −4° incidence

is that the difference in density of the image is potential to the derivative of gradient in refractive index in the field. Using nanopulser as a light source and a parabolic mirror of 80 inch focal length, shadowgraphs are relatively easy to produce. Figure 5 shows the setup to perform shadow photography. Parallel light rays reflecting from the parabolic mirror is passed through the cascade and the image is captured on a Polaroid type 57 film.

Another method of visualizing cascade flows is to coat the cascade with a mixture of dye and oil. Flow field in the cascade is investigated after the tunnel is run for a certain exit Mach number. The pattern formed by the mixture on the blades and end walls is used to interpret the flow behavior.

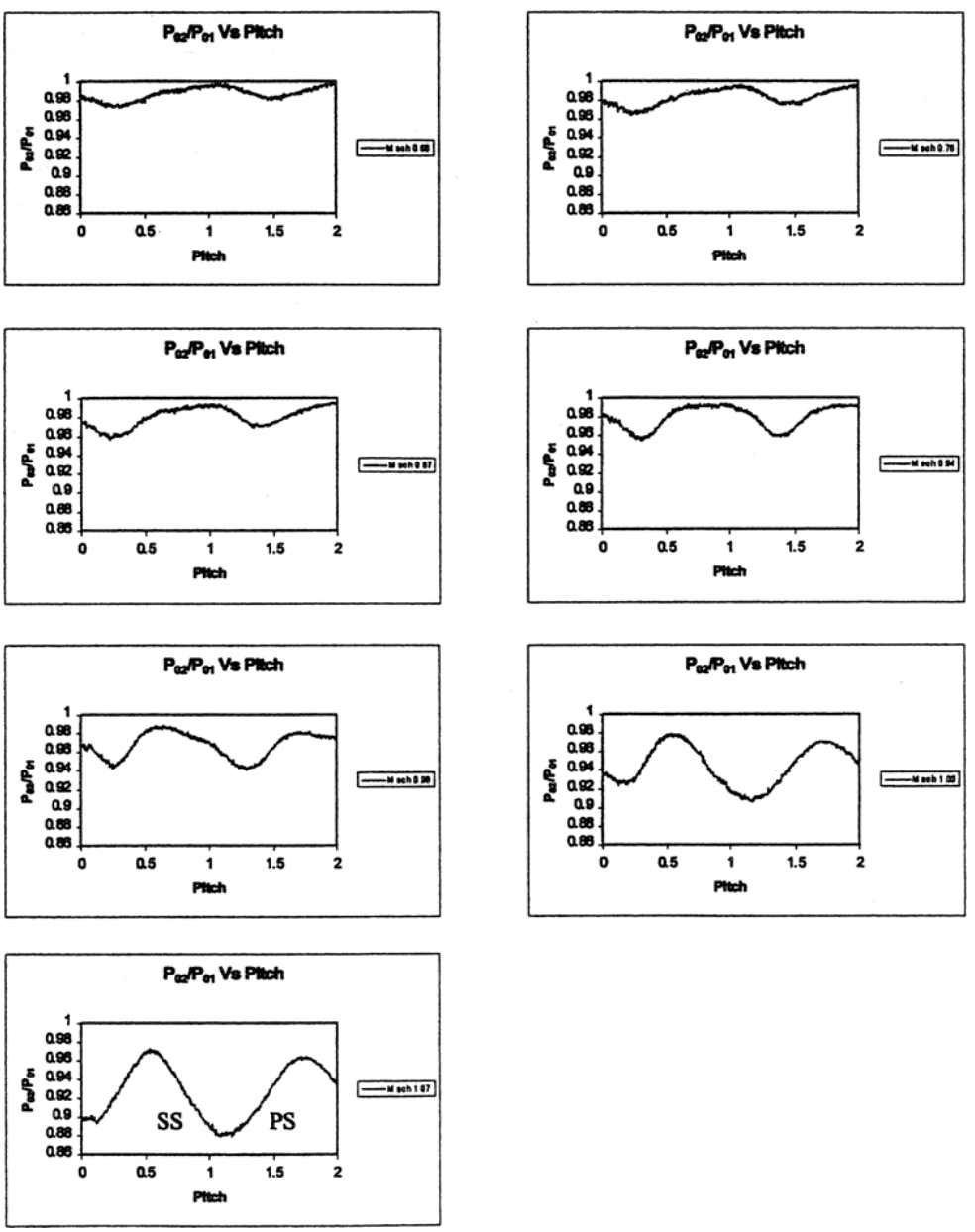

Fig. 8 Pressure ratio at −34° incidence

Oil flow visualization is extremely helpful in investigating the effects of secondary flow in the cascade. In addition it clearly displays discontinuities such as flow separation and shock location. This form of flow visualization also aids in explaining flow data obtained through aerodynamics measurements made in the cascade.

7. Results and Discussion

The measured downstream total pressure profile is normalized with the upstream total pressure to obtain the pressure ratio. The pressure ratio plots vary with pitch that is non-dimensionalized by the traversed distance over the length of the blade passage. These pressure ratio plots display the patterns and periodicity of the flow in two blade passages. A picture of the endwall oil flow visualization is shown in Fig. 6 for $i=-4°$ and the exit Mach number of 0.6. Figure 6 clearly show the periodicity of the exit flow. Figure 7 through 9 display the pressure ratio plots for incident angles $-4°$, $-34°$, and $26°$ at various exit Mach numbers. From the five pressure ratio plots at $-4°$ incidence (Fig. 7), it is evident that the pressure ratios in the free stream and in the wake decrease with increasing exit Mach numbers. The periodicity of the exit flow seems to be good up until exit Mach 0.9. At $-34°$ incidence (Fig. 8), the wake profile is not symmetrical about the wake center at subsonic exit Mach numbers. This is caused by the pressure side separation. This trend changed as the exit Mach number approaches unity and normal shocks start to form at the trailing edge. Stronger shocks have developed across the throat at the trailing edge of the blade originating from the pressure side and impinging onto the suction of the next blade. Flow entering the blade passage at positive incidence of 26° has significant lower pressure ratio

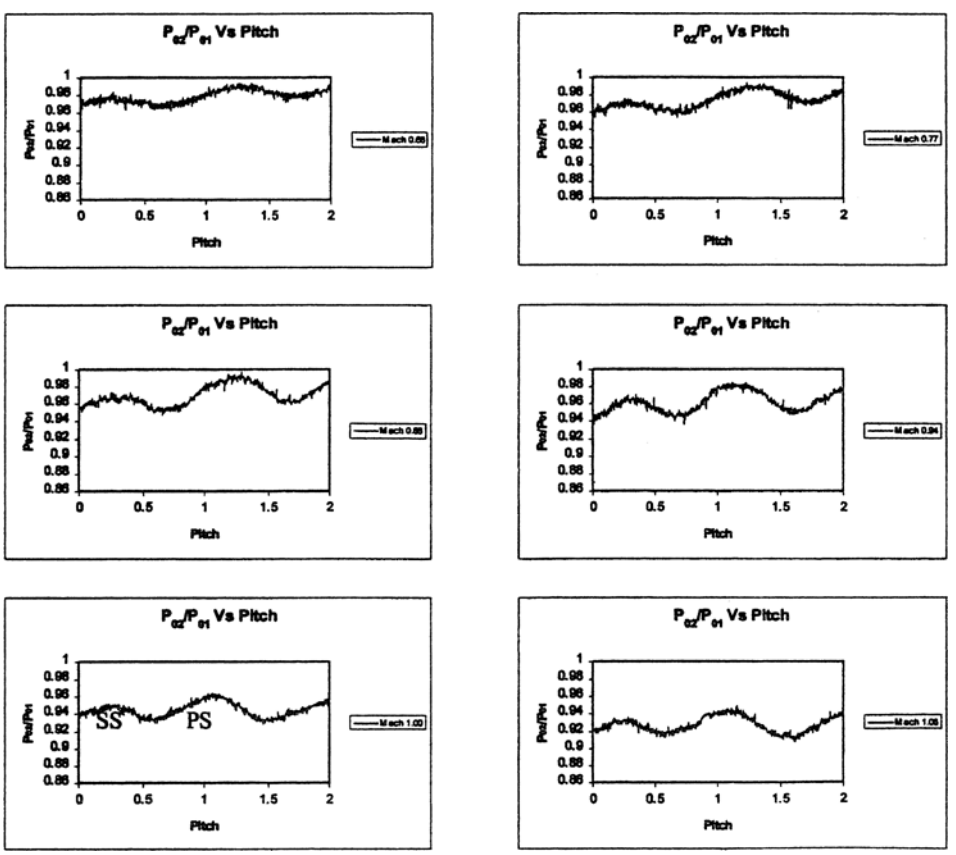

Fig. 9 Pressure ratio at 26° incidence

than at the other two incidences at similar exit Mach numbers (Fig. 9). Even at subsonic exit Mach number of 0.66, there is a 1 % loss in the free stream. Shadowgraphs taken at various exit Mach numbers (Fig. 10) show the progress of shock development and shock induced flow separation to be the dominating factors in creating such low pressure ratios.

The pressure loss coefficient plot with variation in exit Mach number is shown in Fig. 11. The pressure loss coefficient trend can be categorized into three regions. In a subsonic flow at exit Mach number below 0.9, the pressure loss coefficient is dominated by viscous losses, and losses are expected to be rather insensitive to exit Mach numbers. From 0.9 to Mach 1.0, the presence of strong normal shocks causes the pressure loss coefficient to increase at a steep gradient. This is referred to as the transonic region. When the normal shocks turn into weaker oblique shocks in supersonic flow, the pressure loss coefficient will peak in the region of exit Mach 1.1-1.2 and subsequently decrease at higher Mach numbers until the formation of stronger oblique shocks. This is referred to as the supersonic region. The

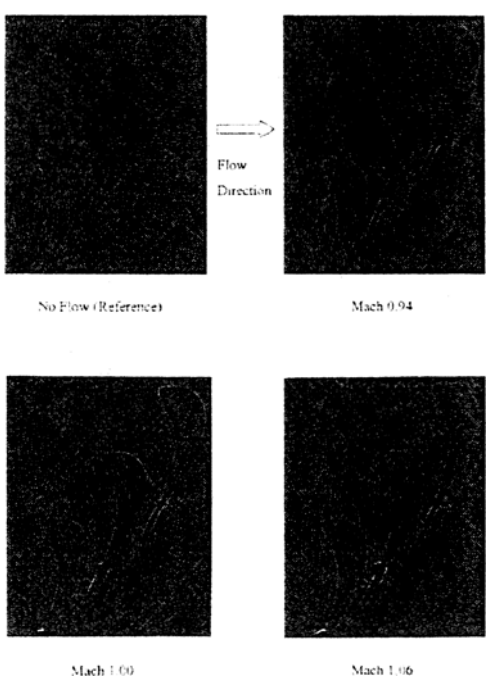

Fig. 10 Shadowgraphs at 26° incidence

trend of the pressure loss coefficient variation with exit Mach number is quite similar at all three incident angles tested. The pressure loss coefficients do not vary significantly with exit Mach number until exit Mach 0.95. At $-4°$ incidence, the pressure loss coefficient increased from 1.1% to 2.5% with exit number from 0.69 to 0.9. This gradual increase is mostly due to higher viscous losses at higher exit Mach numbers as the blade passage is convergent. At subsequently higher exit Mach numbers, the pressure loss coefficient increased steeply due to the formation of normal shocks at the trailing edge. The pressure loss coefficient plateau at exit Mach 1.03 with a value of 6.1%. This suggests that the normal shocks are being transformed into weaker oblique shocks justified by the pressure loss coefficient at exit Mach 1.14 to be around 6%. Mee et al. (1990) and Chen(1987) also observed the peak losses between exit Mach 1.0 to 1.1.

The pressure loss coefficient at $-34°$ incidence behaves closely to that at $-4°$ incidence in subsonic exit flow. Once the exit Mach number is 1.07, the pressure loss coefficient for $i=-34°$ exceeds the pressure loss coefficient at near design ($i=4°$). Together with the shock induced flow separation at the trailing edge, normal shocks are major factors increasing the loss. Due to limitation of the facility, no data are obtained at higher exit Mach numbers. Hence it cannot be concluded whether the loss coefficient will peak at this incidence.

The pressure loss coefficients evaluated at 26° incidence possessed significantly higher losses than near the design incidence in subsonic flow. At exit Mach number of 0.66, the loss coefficient is 2% compared to 1.2% at $-4°$ incidence.

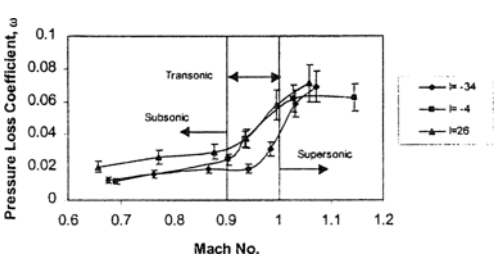

Fig. 11 Pressure loss coefficient variation with exit Mach number and incidence, blade 526A

This difference may be attributed to the leading edge flow separation on the suction surface and the subsequent formation of turbulent boundary layer after reattachment. With flow entering the blade passage at extreme positive incidence, the blade loading is high, causing a region of adverse pressure gradient to be formed on the suction surface. The losses at this incidence increased steeply starting from exit Mach number of 0.93. The loss coefficient increased to 8.6% at exit Mach number of 1.06 and this loss is 18% greater than the loss computed at $-4°$ incidence and 3% greater than the loss at $-34°$ incidence. Trailing edge flow separation and shock-boundary layer interaction are the key components in escalating the loss at supersonic Mach numbers.

8. Conclusions

The influence of extreme flow incidence and Mach number on profile losses is investigated for steam turbine nozzle. The inlet flow incidences are varied from $-34°$ to $26°$ for the cascade and the exit Mach number ranged from 0.6 to 1. 15. Trends for profile loss variation with exit Mach numbers are similar at all tested angles. Losses are constant at subsonic Mach numbers due to an accelerating flow and a thin boundary layer caused by a favorable pressure gradient. In transonic flow the profile losses increase steeply due to the formation of trailing edge shocks and shock induced boundary layer separation. When the exit flow goes supersonic, the losses peak and decrease subsequently due to the transformation of the stronger normal shock into weaker oblique shocks. At subsonic Mach numbers, the profile loss at near design incidences is always the lowest. Losses at extreme positive incidence are always the highest and the periodicity in the flow is the worst. At higher Mach numbers in transonic flow, the losses at off-design incidence is lower than that at the design incidence. This trend is attributed to delayed formation of shocks and subsequent boundary layer separation at high Mach number. When the exit flow goes supersonic in the Mach number range of 1.05 to 1.10, the losses at all incident angles have similar magnitudes. Shadowgraphs show that at those exit Mach numbers, the shock structure at all angles look more developed and somewhat similar.

References

Ainley, D. G., 1948, "The Performance of Axial Flow Turbines," *Proceedings of the Institution of Mechanical Engineers*, Vol. 159

Chen, S., 1987, "A Loss Model for the Transonic Flow Low-Pressure Steam Turbine Blades," *Institute of Mech. Engrs*. C269

Goobie, S., Moustapha, S. H., and Sjolander, S., A., 1989, "An Experimental Investigation of the Effect of Incidence on the Two-Dimensional Performance of an Axial Turbine Cascade," *ISABE* Paper No. 89-GT-188

Hodson, H. P., and Dominy, R. G., 1986, "The Off-Design Performance of a Low Pressure Steam Turbine Cascade," *ASME* Paper No. 86-GT-188

Lakshminarayana, B. 1996, *Fluid Dynamics and Heat Transfer of Turbomachinery* New York : John Wiley & Sons.

Mee, D. J., Baines, N. C., Oldfield, M. L. G., and Dikens, T. E., 1990, "An Examination of the Contributions to Loss on a Transonic Blade Cascade," *ASME* Paper No. 90-GT-264

Venkatrayulu, N., Dasgupta, A., and Srivastava, K. M., 1989, "Studies on the Influence of Mach number on Profile Losses of a Reaction Turbine Cascade," *ISABE* Paper No. 89-7016